DESIGN OF AN AXIAL TURBINE FOR EXCESSIVE PRESSURE RECOVERY IN SMART WATER DISTRIBUTION SYSTEMS

Jiří BEZDÍČEK

V. Kaplan Department of Fluid Engineering, Faculty of Mechanical Engineering, Brno University of Technology, Technická 2896/2, 61699 Brno, Czech Republic

Pavel RUDOLF

V. Kaplan Department of Fluid Engineering, Faculty of Mechanical Engineering, Brno University of Technology, Technická 2896/2, 61699 Brno, Czech Republic

Daniel HIMR

V. Kaplan Department of Fluid Engineering, Faculty of Mechanical Engineering, Brno University of Technology, Technická 2896/2, 61699 Brno, Czech Republic

David ŠTEFAN

V. Kaplan Department of Fluid Engineering, Faculty of Mechanical Engineering, Brno University of Technology, Technická 2896/2, 61699 Brno, Czech Republic

Daniel PATAUNER

Research Group, Fluid-Flow Machinery, Institute for Energy Systems and Thermodynamics, TU Wien, Getreidemarkt 9/302, 1060 Vienna, Austria

Eduard DOUJAK

Research Group, Fluid-Flow Machinery, Institute for Energy Systems and Thermodynamics, TU Wien, Getreidemarkt 9/302, 1060 Vienna, Austria

ANNOTATION

The ongoing digital transformation of water distribution systems necessitates a sustainable and efficient energy source. Traditional systems employ pressure reduction valves (PRVs) to manage excess pressure, a method that unfortunately dissipates potential energy as heat. This study proposes the design of an axial turbine as a novel substitute for PRVs, aiming to recover this otherwise wasted energy. The axial turbine design, encompasses an innovative variant featuring counter-rotating runners. This design is geared towards harnessing energy from excess pressure, thus generating electricity. This electricity can then power the digitalization of the network and cater to its self-consumption needs, promoting a self-sustaining infrastructure. This research contributes to the development of smarter, more sustainable water management practices by integrating energy recovery into system architecture, aligning with broader environmental and economic goals.

KEY WORDS

Energy recovery, Water Distribution networks, Axial Turbine, Shape optimization.

1. INTRODUCTION

Water distribution networks (WDNs) are a well-known candidate for recovery of surplus energy and energy harnessing. It is necessary to carry out an in-depth analysis of the WDN beforehand. The foremost aspect is to identify suitable locations of exploitable hydro-potential before selecting particular type of device. Locations with reasonable potential can be equipped with conventional devices, most commonly Pump in Turbine mode (PaT) or axial turbines.

In some networks, specific conditions can occur that may result in selection of equal pressure devices such as Pelton turbine or Cross Flow turbines. These devices have the disadvantage of an atmospheric pressure value at their outlet which may not be sufficient for further water transport. Designs of other unconventional recovery devices, such as Sinagra´s internal CrossFlow turbine [1] or lift-based turbines [2], also appear in the literature.

This paper is aimed on design of axial turbine for given site in Austrian WDN, where beneficial pressure and discharge conditions were found for energy recovery. The choice of the axial turbine was made considering not only the specific pressure and discharge conditions but also the dimensional and technical layout of the site. Furthermore, relatively new concept of counter – rotating runners was adopted. For the same application, this principle was investigated by Biner [3].

2. INVESTIGATED WATER DISTRIBUTION NETWORK (WDN)

From the measurements made on a typical summer day in the investigated site, it was found that the pressure and flow patterns are almost constant. This effect is mainly due to the location of the valve in front of the storage tank.

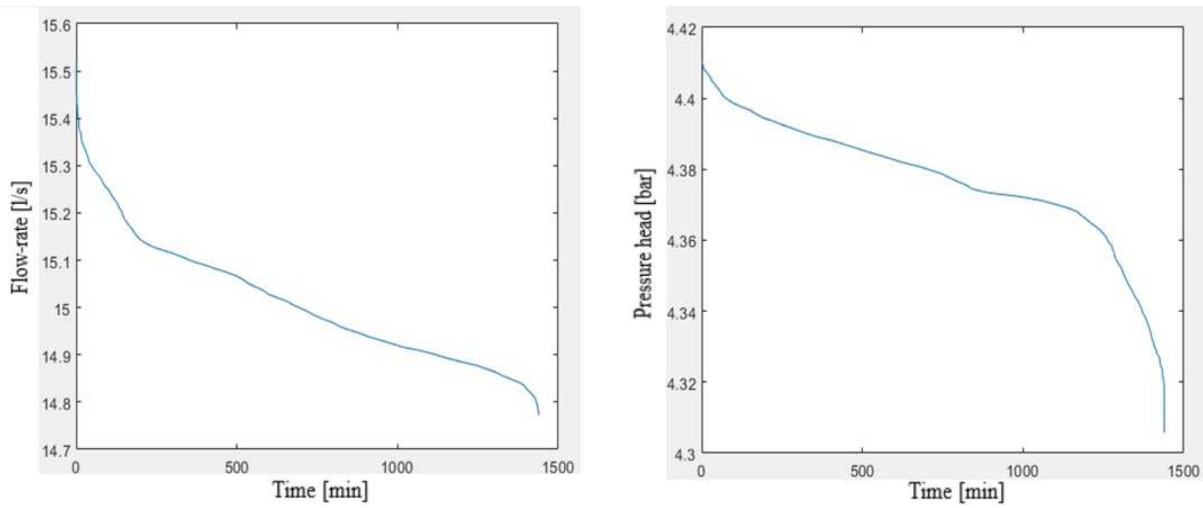

Figure 1 Pressure and flow duration curves

In this case, the classical methodology of subtracting design parameters from duration curves of one year was also applied to time course data of measured quantities from one day. The described methodology led to a design head of H = 44.88 m and a discharge of Q = 15 l/s. Another aspect is the geometric layout of a given PRV site within which the valve is to be replaced by a recovery device. The pipeline here reaches a clearance of DN100 and it was further determined that the turbine should not have a overall depth of blade cascades greater than 1 m.

3. INITIAL DESIGN PROPOSAL

Since it was determined that the ideal candidate for energy recovery at the specified location is an axial turbine, it is still necessary to estimate its initial dimensions based on hydraulic, geometric and electrically related dispositions. The first important parameter is the choice of nominal speed. The synchronous speed can be determined according to the following relationship:

$$p \cdot n = f \cdot 60 \tag{1}$$

Where: p is number of pole doubles, f is frequency of the power grid (for Austria 50 Hz.). Nominal speed should be also selected so that the designed machine is hydraulically most advantageous. It is the hydraulic aspect that can be expressed by the specific speed criterion.

$$n_s = 3.65 \cdot n \cdot \frac{Q^{0.5}}{H^{0.75}} \tag{2}$$

If the parameter p = 1 is considered, the synchronous speed results in 3000 min^{-1}. Considering this speed value together with the design parameters of the head and discharge dependencies leads to specific speed value 77,34 min^{-1}. Since this is a value from the lower end of the specific speed range, increasing the number of poles would result in hydraulically less advantageous hydraulic geometries.

Another aspect is the design of the shroud diameter, given that this is a relatively low specific speed design, smaller turbine diameters will result in higher meridional velocities and consequently more beneficial hydraulic behavior of machine. A shroud diameter of 80 mm was chosen, with the additional advantage of possibility of outlet diffuser design for ideal pressure recovery.

4. GEOMETRY DESIGN AND OPTIMIZATION ON REDUCED CFD MODEL

Since a counter-rotating turbine was chosen, the first stage of the turbine was designed first. The principle of counter-running runners is still in the literature relatively an unexplored solution. For this reason, a “Optimization does it all” design approach was selected. This procedure is described by following *Figure 2*.

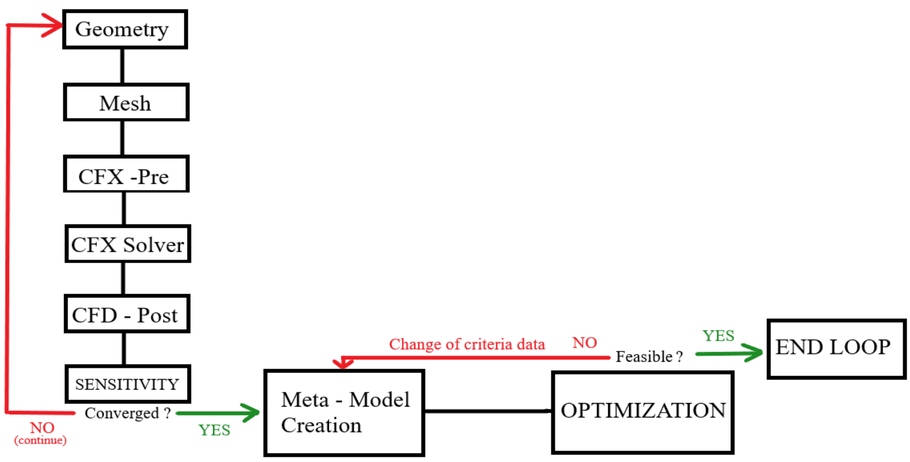

Figure 2 Schematic interpretation of optimization procedure algorithm

A reduced CFD model was created for the defined optimization loop. This simplified set-up consisted of only the first rotor cascade and the inlet and outlet domains, which were simplified to intermediate rings. Second stage (counter runner) was not included in optimization procedure and it was designed by standard semi-empirical methods and included only into final complete CFD model, which was used for consequent validation.

4.1 Initial geometry.

Initial (reference) geometry for optimization procedure was created by standard semi – empirical methods, specifically quadratic change of complementary angle $\bar{\beta}$ in conformal mapping functional space. After creating centerline, NACA 0009 was fitted. Inflection point was prescribed on trailing edge of blade centerline. Design parameters used for reference design as well as considered velocity triangles are shown in the following *Table 1*.

Depth of cascade [mm]	35
Hub radius [mm]	34,4
Shroud radius [mm]	40
Shroud TIP GAP [mm]	0,5
Blade count [-]	5
Predicted efficiency for first stage [%]	85
Design head for first stage [m]	22,5

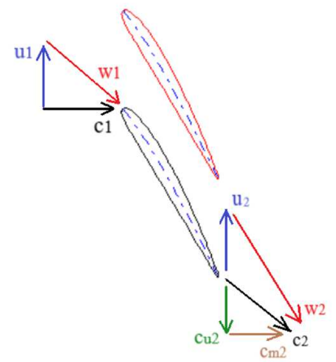

Figure 3 Design velocity triangles for reference geometry

Table 1 Basic dimensions of reference design

The dependence of the Θ angle on the normalized *M-Prime* meridional distance was parameterized, this process is described in Section 4.4. Where *M-Prime* represents normalized meridional distance with respect to particular radius.

4.2 Computational meshes

Intermediate domains were spatially discretized in *Ansys Meshing* software, while for the rotor blade cascade, mesh was created in *TurboGrid* pre-processor. The result was a fully hexahedral computational mesh.

Quality measures		Inlet	Runner	Outlet
Element count · 10^6		0,42	1,16	6,87
Aspect ratio	MIN	5,7	9,6	-
	Average	23,1	39,3	56,3
	Max	11,1	18,8	-

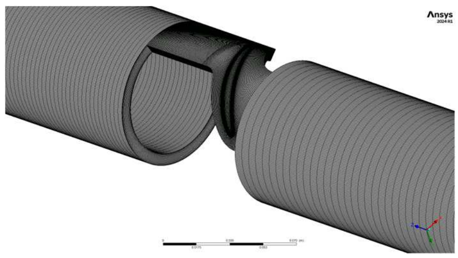

Figure 4 Computational mesh for reduced CFD model

Table 2 Computational mesh quality

4.3 Solver set-up

Ansys CFX 2023 was used as CFD solver for its robustness in turbomachinery computations. The specific solver settings are then shown in the following *Table. 3.*

Turbulence model	SST k - ω	
Interfaces	STAGE	
Boundary conditions	Inlet BC	MassFlow rate
	Outlet BC	Static pressure (patm)
Convergence	Iterations	75-150
	RMS res	10^{-4}

Table 3 CFD solver set-up

RANS approach was chosen, utilizing *SST* $k-\omega$ model with automatic wall functions. Considering this, the y+ was also kept below 1. The STAGE interface model (mixing plane approach) was used to connect the relative rotating coordinate system with its neighbour stationary domains. Selected convergence control was made and tested specially for reduced CFD model, as for standard CFD calculation these values would be insufficient.

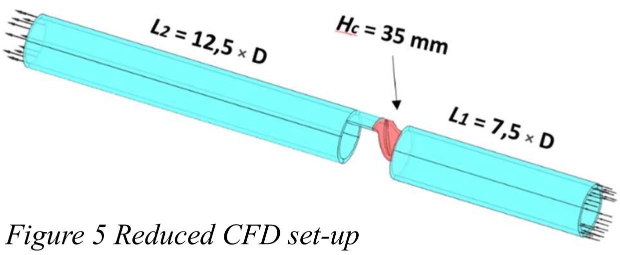

Figure 5 Reduced CFD set-up

Only one blade channel with prescribed rotational periodicity was considered for the steady-state CFD calculations that were used for optimization. Length of outlet and inlet domains is shown in *Figure 5.*

4.4 Sensitivity analysis set-up

Stochastic (sensitivity) analysis was carried out in OptiSlang software. Reference geometry was parametrized by overall 10 design parameters including six parameters prescribed for control points of kubic Bezier curve describing centreline on hub. During run of sensitivity analysis, parametric space was filled according to Advanced Latin Hypercube method. Over-all 423 samples were computed.

Parameter	Minimal value	Maximal value
Hub radius [mm]	32	36
Shroud TIP [mm]	0,3	0,6
Number of blades [-]	3	12
Depth of cascade [mm]	35	70

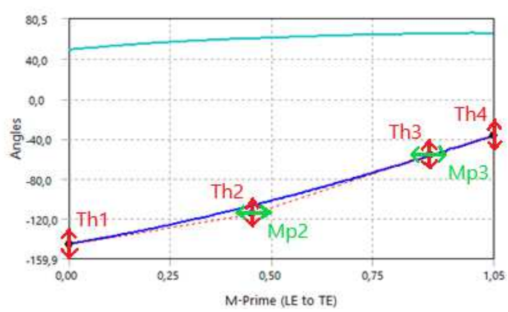

Figure 6 Continuous functional space for stochastic analysis

Table 4 Defined parameters with prescribed

Individual control points were allowed to move ±20 % from their reference value. Where for particular control point *Th* represents movement in the θ coordinate and *Mp* in the meridional direction.

4.5 Meta – model

Sensitivity analysis led to creation of *MetaModel*. Which was used for consequent optimization procedure.

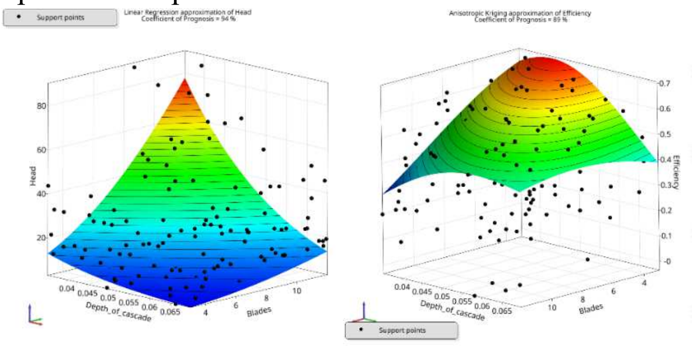

Figure 7 Created response surfaces

As can be seen from the plotted dependencies of the blade cascade depth and blade number parameters, the Head dependence was given by a standard linear regression, while the more complex Anisotropic Kriging model was used for efficiency. Regression quality which is important for consequent optimization was estimated as sufficient.

From sensitivity analysis, best feasible design in terms of efficiency was selected for comparison with final optimized geometry. This design was called *best from stochastic*.

The regression surfaces were further used to observe the effect of each parameter on the defined responses. Important characteristics include, in particular, an increase in head and also an increase in efficiency when reducing the depth of the blade cascade while maintaining the same wrap angle. Another expected behavior for pre-chosen design is increase in efficiency and decrease of head while decreasing number of blades. These effects were used to create final design, as it is described in chapter 6.1.

4.6 Optimization (*MetaModel* based)

A genetic algorithm (*GA*) was used for optimization with the implementation of an evolutionary strategy (*ES*) whose role was to find the local minimum, since *GA* is mainly suitable for global search of the function space. Same objective functions were used as in case of sensitivity analysis. Following set – up of population was made:

Maximum samples	Start population size	Population size	Maximum generations	Stagnation generations
40 100	300	200	200	20
Archive size	Number of parents	Ranking method	Selection method	-
2	9	Linear	Stochastic	-

Table 5 Population sizes, convergence and selection strategy

After setting basic parameters such as the number of individuals in the population or the selection methodology, the mechanisms of recombination and mutation were further defined. Two crossover methods were used for recombination procedure. The first is the frequently used uniform recombination, while the simulated binary method was further defined. A 50% recombination probability was defined for each of these methods. Normal distribution with 11% mutation probability was used for the mutation. Since single objective function optimization approach was adopted, only one design is output from the optimization itself.

5. COMPLETE CFD MODEL

Complete CFD model was used for validation of previous results from reduced model and optimization results. The complete model considered not only the inlet and outlet domains with stationary hubs but also the second stage of the turbine, which was designed based on the CFD results of the first stage.

5.1 Design of counter runner

The second stage was designed using standard semi-empirical methods. The main purpose of the second stage is to process the flow from the first stage and minimize the c_u component at the outlet of the turbine. With this in mind, the basic design parameters were chosen, such as the depth of the blade cascade, which was set to 70 mm.

As the first runner was designed for approximately half the head, it is necessary that the counter – rotating stage process sufficient residual head to ensure that the complete turbine meets the design parameters. The Euler turbine equation shows that the value of the head in the case of this stage is limited by the energy (magnitude c_u velocity component) generated by the first wheel.

The Euler turbine equation in its standard form is defined as follows:

$$g \cdot H \cdot \eta_T = u_1 \cdot c_{u1} - u_2 \cdot c_{u2} \tag{5}$$

If we consider: $c_{u2} = 0$; $u_2 = u_1 = \pi \cdot Ds \cdot n$; $\eta_T = 0{,}7$

Where H is head. $u_2 = u_1$ is peripheral velocity, Ds is diameter of the middle stream-surface (SPAN 05) and $\eta_T = 0{,}7$ is predicted efficiency. We can establish the following relation for predicted available head:

$$H = \left(\frac{1}{tg\,\beta_1} + \frac{u_1}{c_{m1}}\right) \cdot \frac{c_{m1} \cdot u_1}{g \cdot \eta_T} \tag{6}$$

Where β_1 is inlet angle at counter – stage and c_{m1} is meridional velocity. These quantities were subtracted from the flow-field of the reduced CFD model of each selected variant.

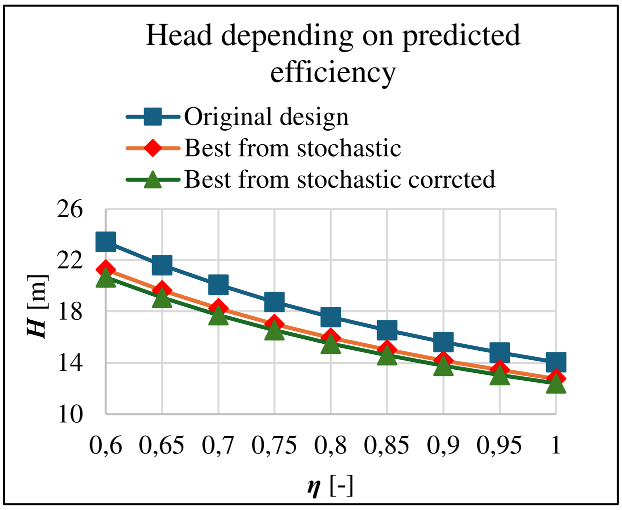

Based on this analysis and the quantification of the results from the reduced CFD model at the outlet of the first stage, second stage blade cascade was designed for each of first stage variants. The final corrected design was designed with the inlet angle $\overline{\beta_1}$ set to -3.5° and the angle $\overline{\beta_2}$ to suppress c_u velocity component at outlet. In this case, a quadratic change of the $\overline{\beta}$ angle was performed again. Hub radius and shroud TIP Gap value was defined to match fisrst stage variant. Every version of second stage runner had nine blades.

5.2 Inlet and outlet domain

The input converging domain is 0.14 m long to ensure that the convergence angle was kept as low as possible to suppress instabilities. A standard divergence angle value of 12° was selected for the diffuser. Another component was the upstream and downstream struts, the purpose of which is to attach the stationary hubs to the pipe system.

<table>
<tr><th colspan="4">Additional computational meshes for complete CFD model</th></tr>
<tr><td rowspan="2">Inlet converging part</td><td>Number of elements $\cdot 10^6$</td><td>3,09</td><td rowspan="2">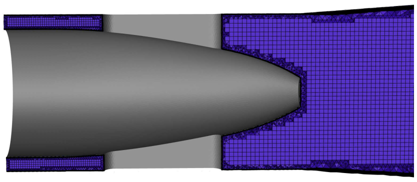
Figure 8 Detail of computational mesh of converging section</td></tr>
<tr><td>Average orthogonality</td><td>0,873</td></tr>
<tr><td rowspan="2">Outlet diffuser</td><td>Number of elements $\cdot 10^6$</td><td>3,09</td><td rowspan="2">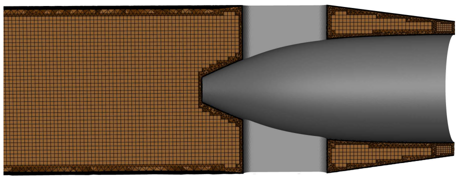
Figure 9 Detail of computational mesh of outlet diffuser</td></tr>
<tr><td>Average orthogonality</td><td>0,864</td></tr>
<tr><td>Swirl runner</td><td>Number of elements $\cdot 10^6$</td><td>3,8</td><td>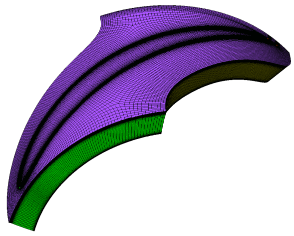
Figure 10 Computational mesh of first stage of turbine (swirl runner)</td></tr>
<tr><td>Counter runner</td><td>Number of elements $\cdot 10^6$</td><td>1,8</td><td>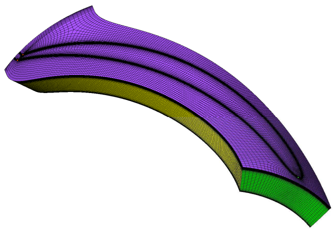
Figure 11 Computational mesh of second stage of turbine (counter runner)</td></tr>
</table>

Table 6 Computational meshes for complete CFD model

5.3 Solver set-up

The solver setup was performed identically to the reduced model. The difference is in addition of another stage interface which is placed between runners and also higher requirements for the convergence criteria were defined. Requested RMS residuals were 10^{-5} and minimum number of iterations was set to be 500.

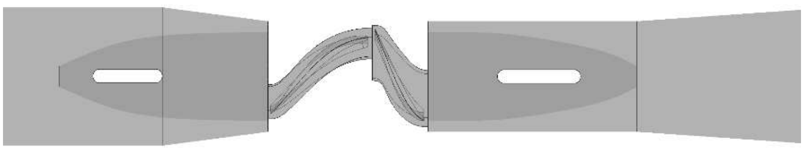

Figure 12 Complete fluid domain for CFD validation

6. RESULTS

In this chapter, three designs that emerged from stochastic analysis and optimization were compared. Comparison was done in terms of qualitative assessment of flow-field but also from perspective of integral characteristics.

6.1 Basic dimensions of first stage designs.

During optimization process three designs were created. First called *Best from stochastic* is selected best feasible design from computed design points of sensitivity analysis. Subsequently, the design was obtained directly from the optimization that was performed on the created *MetaModel*, this design was named *Optimized*. Finally after compering results of these geometries with original geometry, design *Best from stochastic corrected* was created by manual adjustments of *Best from stochastic* design according to observed trends from response surfaces, specifically number of blades and depth of cascade was adjusted. Main purpose of conducted correction was to satisfy Rotor-Stator interaction (*RSI*) theory.

Proposed design	Depth of cascade [mm]	Hub Radius [mm]	Number of blades [-]	Shroud Tip Gap [mm]	Wrap angle (on HUB)
Original design	35	33,4	5	0,5	108,4
Best from stochastic	39,5	32	6	0,58	111,41
Optimized	60,85	32,5	10	0,5	115,50
Best from stochastic corrected	35	32	5	0,58	111,41

Table 7 Basic dimensions of proposed designs in comparison with original design

6.2 Comparison of proposed designs.

The following table contains the head and efficiency values for first stage of turbine. The results from each computational procedure, i.e., optimization results, CFD data from the reduced model and the evaluated quantities at the first stage of the turbine from the complete CFD model were presented.

Design		Best from stochastic	Optimized	Best from stochastic corrected
Optimized results	H [m]	-	23,01	-
	η [%]	-	70,73	-
Results from reduced CFD	H [m]	22,26	24,00	24,70
	η [%]	68,58	67,53	62,00
Results from complete CFD	H [m]	20,92	37,29	23,09
	η [%]	71,66	55,25	68,59

Table 8 Results comparison for first stage of turbine

The highest first-stage efficiency is achieved by the *best from stochastic variant*, which corresponds to the feasible design with the highest efficiency from the sensitivity analysis. However, this variant is disadvantageous in terms of Rotor-Stator Interaction (RSI) since, as already mentioned, all counter-rotating runner variants had 9 blades. Thus it results in dynamically inconvenient configuration. Based on above results, corrected design was selected as final first stage geometry.

6.3 Qualitative analysis of flow-field from complete CFD model.

For qualitative analysis, results from complete CFD model were used. This analysis was carried out mainly for validation of final designs and is not aimed as in-depth analysis of flow in proposed turbine. To investigate no-shock inflow on blade cascades, detachment of flow and other phenomena in blade channels, the streamlines relative velocity were plotted for each investigated variant.

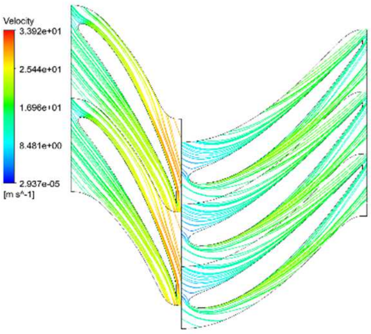

Figure 13 Streamlines on complete domain of turbine variant: best from stochastic

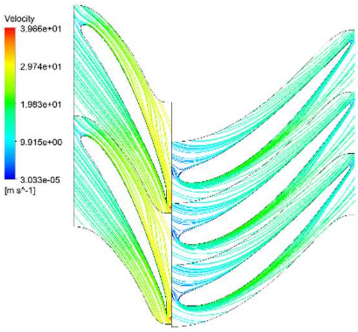

Figure 14 Relative velocity streamlines, variant: best from stochastic corrected

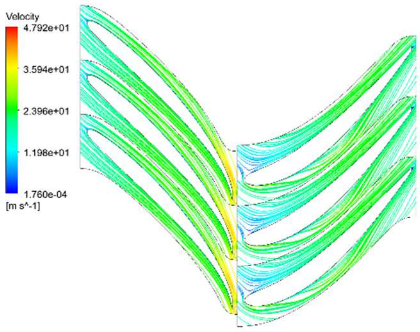

Figure 15 Relative velocity streamlines, optimized variant

It is apparent that no-shock inflow was maintained for every designed first stage. Second stage of *best from stochastic design* was also without shock inflow. For corrected design as well as design from optimization, small incidence on pressure side of blade was allowed.

Achieving axial flow at the outlet of the turbine energy regions, i.e. the ability of each variant to minimize the cu component at the outlet, was also verified.

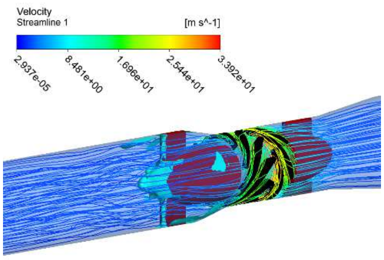

Figure 16 Relative velocity streamlines variant: best from stochastic

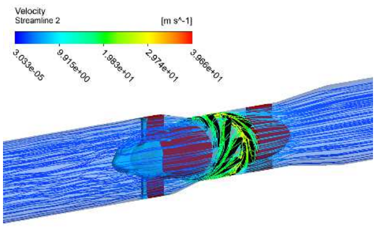

Figure 17 Streamlines on complete domain of turbine. best from stochastic corrected

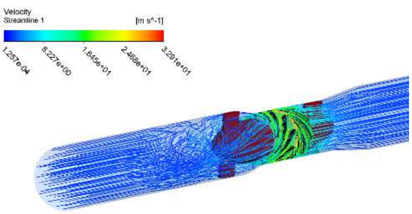

Figure 18 Streamlines on complete domain of turbine, optimized variant

Axial outflow was reached for both variants coming from stochastic analysis. It is also visible that backflow area visualized by stagnation iso-surface is relatively small and located around axis, where this phenomena is expected. For optimized variant, axial outflow was not reached, this variant was not further investigated due to excessive head, caused by very dense blade cascade.

Finally, turbine characteristics of final variant were obtained. Off-design regimes were computed on complete CFD model of corrected design, which was selected as final solution. Not only the n_{11} range corresponding to the measured data was investigated, but also off-design regimes from a wider n_{11} range for a further assessment of the behavior of the proposed turbine.

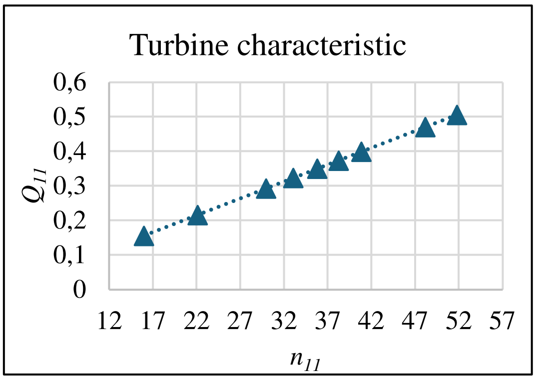

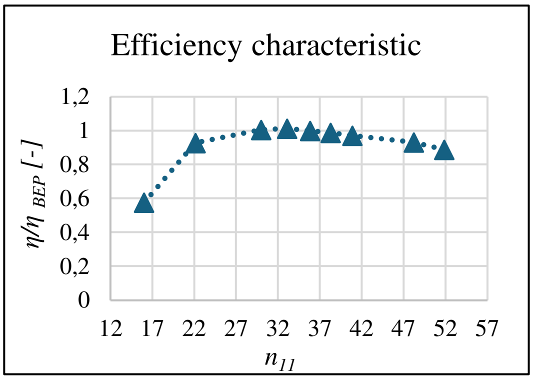

Range (16 - 52) of unit speed $\boldsymbol{n_{11}}$ was investigated. Linear dependency of unit discharge Q_{11} on n_{11} was achieved. Turbine has relatively flat hydraulic efficiency characteristic from 30 % partload to 140 % overload of design point discharge.

7. CONCLUSION

An axial turbine based on the principle of counter-rotating impellers was developed to recover surplus energy from a specific location in the water supply network in Austria. The turbine was subjected to shape optimization using a robust sensitivity analysis to obtain the response surfaces on which the shape optimization was subsequently performed. Combination of genetic algorithm and evolutionary strategy was used as the selected algorithm. The result is proposal of three different designs, two obtained from sensitivity analysis and one is the output of the optimization. For the selected final design, turbine characteristics were obtained by CFD calculations. Linear dependency of turbine characteristic was reached while hydraulic efficiency characteristic is sufficiently flat for operation in given locality.

8. ACKNOWLEDGEMENT

This publication is based upon project TK70020001 "Digitalization of water supply infrastructure to optimize the Water-Energy nexus" (Technology Agency of the Czech Republic) and work from COST Action "Pan European Network for Sustainable Hydropower"; (PEN@Hydropower) CA21104
supported by COST (European Cooperation in Science and Technology)

9. REFERENCES

*[1] SINAGRA, Marco, et al. A new device for pressure control and energy recovery in water distribution networks. Water, **2017**, 9.5: 309.*

[2] DIAB, Ghada; ELHAKEEM, Mohamed a SATTAR, Ahmed M.A. Performance assessment of lift-based turbine for small-scale power generation in water pipelines using OpenFOAM. Online. Engineering applications of computational fluid mechanics. 2022, roč. 16, č. 1, s. 536-550. ISSN 1994-2060. Dostupné z: https://doi.org/10.1080/19942060.2021.2019129.

[3] Biner, D.; Hasmatuchi, V.; Rapillard, L.; Chevailler, S.; Avellan, F.; Münch-Alligné, C. DuoTurbo: Implementation of a Counter-Rotating Hydroturbine for Energy Recovery in Drinking Water Networks. Sustainability ***2021**,* 13, *10717. https://doi.org/10.3390/su131910717*